

Supplementary Materials for

Carbon-free H₂ production from ammonia triggered at room temperature with an acidic RuO₂/γ-Al₂O₃ catalyst

Katsutoshi Nagaoka, Takaaki Eboshi, Yuma Takeishi, Ryo Tasaki, Kyoko Honda, Kazuya Imamura, Katsutoshi Sato

Published 28 April 2017, *Sci. Adv.* **3**, e1602747 (2017)
DOI: 10.1126/sciadv.1602747

This PDF file includes:

- Procedures for characterizing the catalysts
- fig. S1. Conversions and yields for oxidative decomposition of ammonia (Eq. 2) calculated from thermodynamics with HSC Chemistry 6.1.
- fig. S2. Characterizations of RuO₂/γ-Al₂O₃.
- fig. S3. Typical experimental procedure for triggering tests using heat produced by adsorption of ammonia on the catalyst.
- fig. S4. Schematic of the quasi-adiabatic reactor with a quadrupole mass spectrometer (Q-MS) and gas chromatograph (GC).
- fig. S5. Experimental setup for observing the temperature distribution of the catalyst bed.
- fig. S6. Trends of MS peak intensities during triggering tests over RuO₂/γ-Al₂O₃ (A) and bare γ-Al₂O₃ (B).
- fig. S7. Triggering tests over RuO₂/γ-Al₂O₃ with three GHSVs.
- fig. S8. Distribution of catalyst bed temperature measured at 300 s during triggering tests over RuO₂/γ-Al₂O₃ with three GHSVs.
- fig. S9. NH₃-TPD profiles of RuO₂/γ-Al₂O₃ (solid lines) and bare γ-Al₂O₃ (dashed lines).
- fig. S10. Experimental procedure used for five cycles of testing.
- table S1. Conversions of ammonia and oxygen and yields of hydrogen during triggering tests over RuO₂/γ-Al₂O₃ at three GHSVs.
- table S2. Proportions of converted NH₃ and O₂ and percentage yields of hydrogen during triggering tests over RuO₂/γ-Al₂O₃ with various NH₃/O₂ molar ratios in the feed gas.
- table S3. Physicochemical properties of the catalysts.

- table S4. Molar ratio of Ru/Al in RuO₂/γ-Al₂O₃ before testing (untreated), after five cycles of testing, and after long-term testing (100 hours).
- Reference (39)

Procedures for characterizing the catalysts

X-ray diffraction analysis was carried out using a SmartLab X-ray diffractometer (Rigaku, Tokyo, Japan) equipped with a monochromatized Cu-K α radiation source. X-ray photoelectron spectroscopy measurements were performed using an ESCA-850 (Shimadzu, Kyoto, Japan). The binding energy was calibrated by assuming the Al 2*p* core level to be 74.7 eV (39). Throughout the measurements, the Al 2*p* peak did not split and retained the same shape. High-angle annular dark-field scanning transmission electron microscopy observations were obtained using a JEM-ARM200F (JEOL, Tokyo, Japan) operated at 200 kV. The samples were dispersed in ethanol, added dropwise to a carbon-coated copper grid, and dried by exposure to air under ambient conditions for 24 h.

Temperature-programmed desorption (TPD) of NH₃ (fig. S9) was performed in a TPD-1-AT apparatus (MicrotracBEL, Osaka, Japan). Catalyst (200 mg) was loaded into a quartz reactor, treated in He at 300 °C for 30 min, and cooled to 50 °C. Subsequently, 5000 ppm NH₃ diluted in He (50 mL min⁻¹) was fed to the catalyst for 30 min at 50 °C; then the oven temperature was increased at 10 °C min⁻¹ to 500 °C. Desorption profiles of NH₃, H₂O, and N₂ were monitored by quadrupole mass spectrometry at *m/e* = 16, 18, and 28, respectively.

The specific surface area of the catalyst after N₂ treatment at 300 °C was determined by the Brunauer-Emmett-Teller method using a BELSORP 18S and a BELSORP-mini (MicrotracBEL, Osaka, Japan).

The CO chemisorption capacity was measured to enable comparison of the Ru dispersion over two different catalysts. Hydrogen was supplied to each sample at 30 mL min⁻¹ during programmed heating of 10 °C min⁻¹ to 400 °C. The sample was maintained at 400 °C for 60

min, purged in He at 400 °C for 30 min, cooled to 0 °C, and finally flushed with He for 60 min. Following pre-treatment, CO chemisorption was carried out at 0 °C in a He stream (30 mL min⁻¹) using a pulsed-chemisorption technique.

Energy dispersive X-ray fluorescence analyses were carried out using an EDXL 300 (Rigaku).

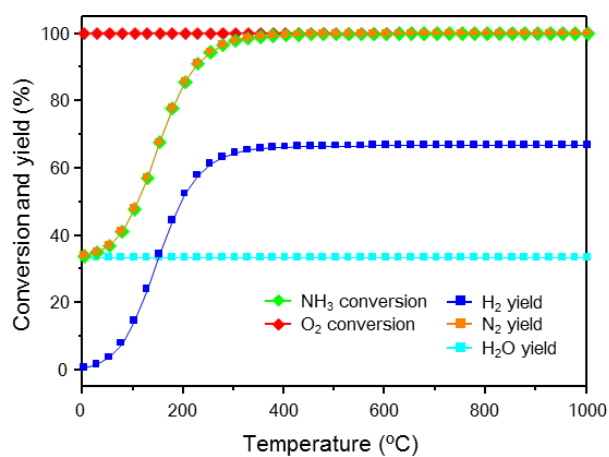


fig. S1. Conversions and yields for oxidative decomposition of ammonia (Eq. 2) calculated from thermodynamics with HSC Chemistry 6.1. (Outotec Research Oy, Pori, Finland).

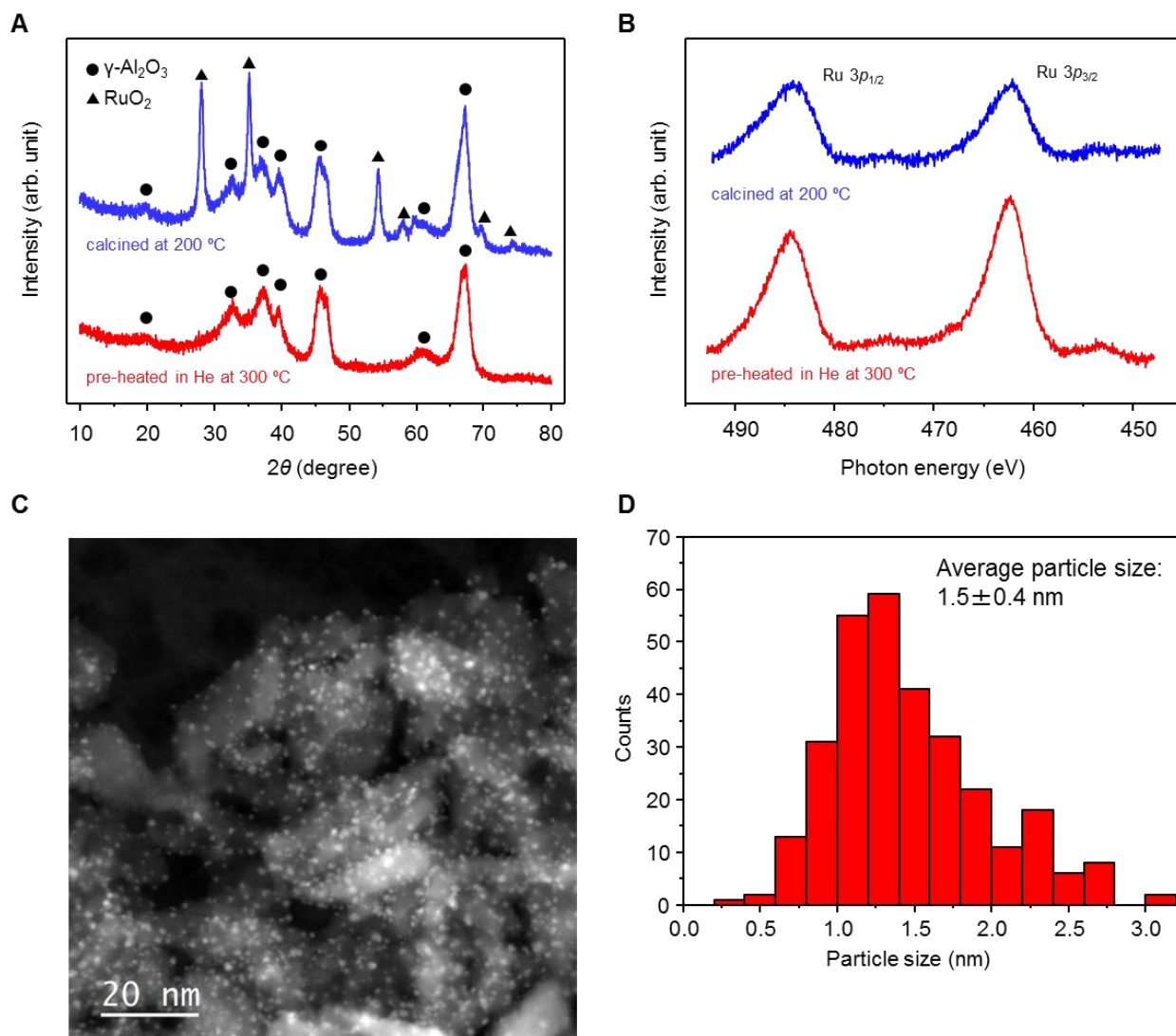


fig. S2. Characterizations of RuO₂/γ-Al₂O₃. X-ray diffraction patterns (A), X-ray photoelectron spectra (B), high-angle annular dark-field scanning transmission electron micrograph of RuO₂/γ-Al₂O₃ (C), and Ru particle size distribution (D).

Because of the widespread dispersion of Ru species on the catalyst, no peaks for Ru species were visible in the X-ray diffraction pattern for the RuO₂/γ-Al₂O₃ synthesized with pre-heating in He at 300 °C (fig. S2A). Diffraction peaks for RuO₂ were observed for RuO₂/γ-Al₂O₃ after calcination at 200 °C in air. The binding energies of Ru 3p in the as-synthesized RuO₂/γ-Al₂O₃ were identical to those of Ru 3p in RuO₂/γ-Al₂O₃ calcined at 200 °C in air (fig. S2B). These results indicate that Ru existed as RuO₂ in both samples. Furthermore, the high-angle annular dark-field scanning transmission electron micrograph (fig. S2C) shows that the mean particle size of RuO₂ was 1.5 ± 0.4 nm (fig. S2D) for the as-synthesized RuO₂/γ-Al₂O₃.

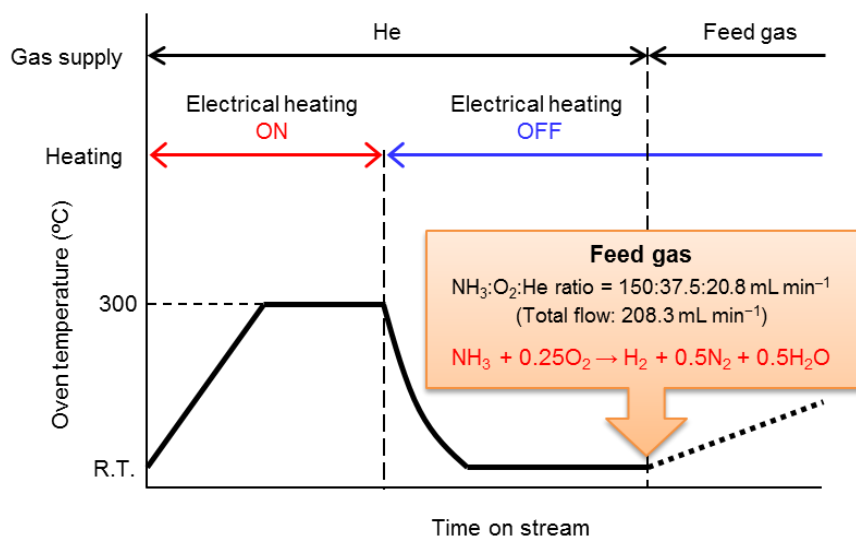


fig. S3. Typical experimental procedure for triggering tests using heat produced by adsorption of ammonia on the catalyst.

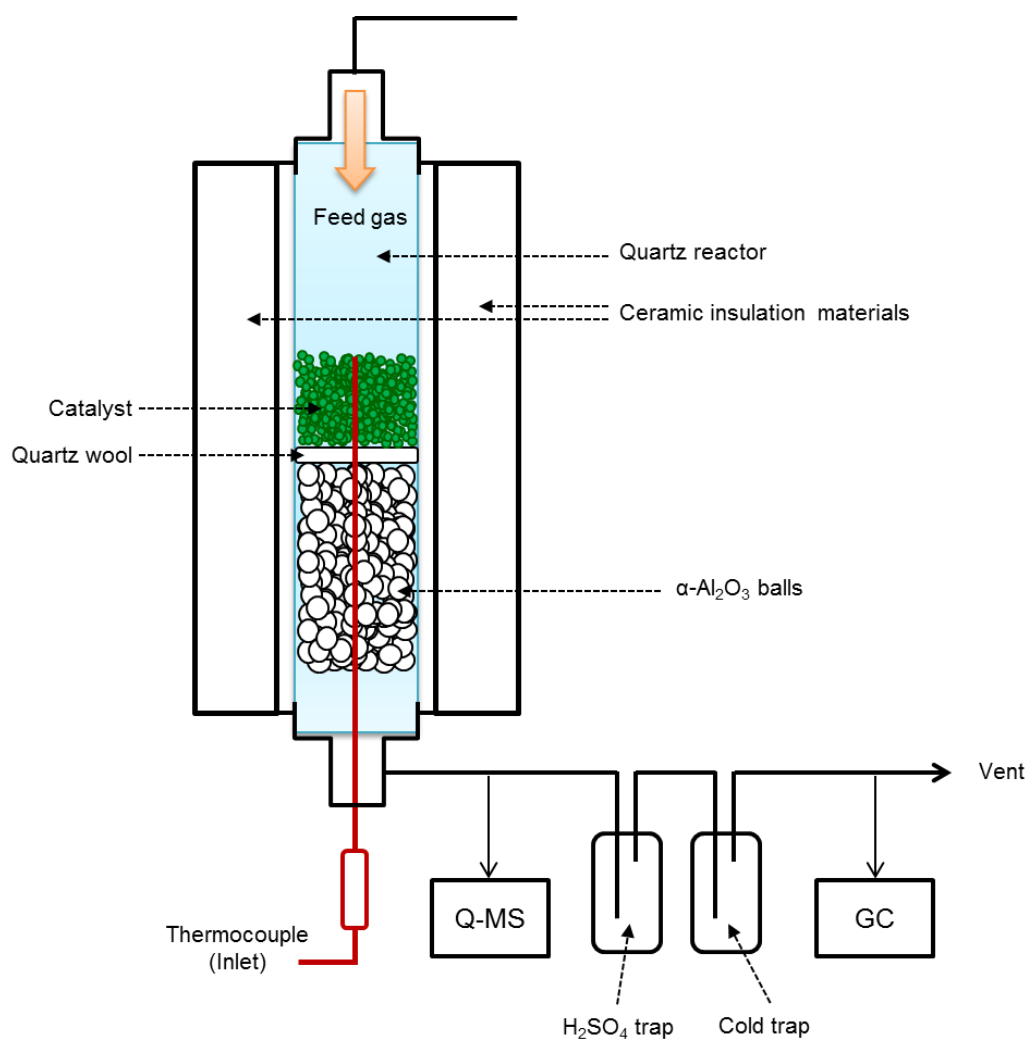


fig. S4. Schematic of the quasi-adiabatic reactor with a quadrupole mass spectrometer (Q-MS) and gas chromatograph (GC).

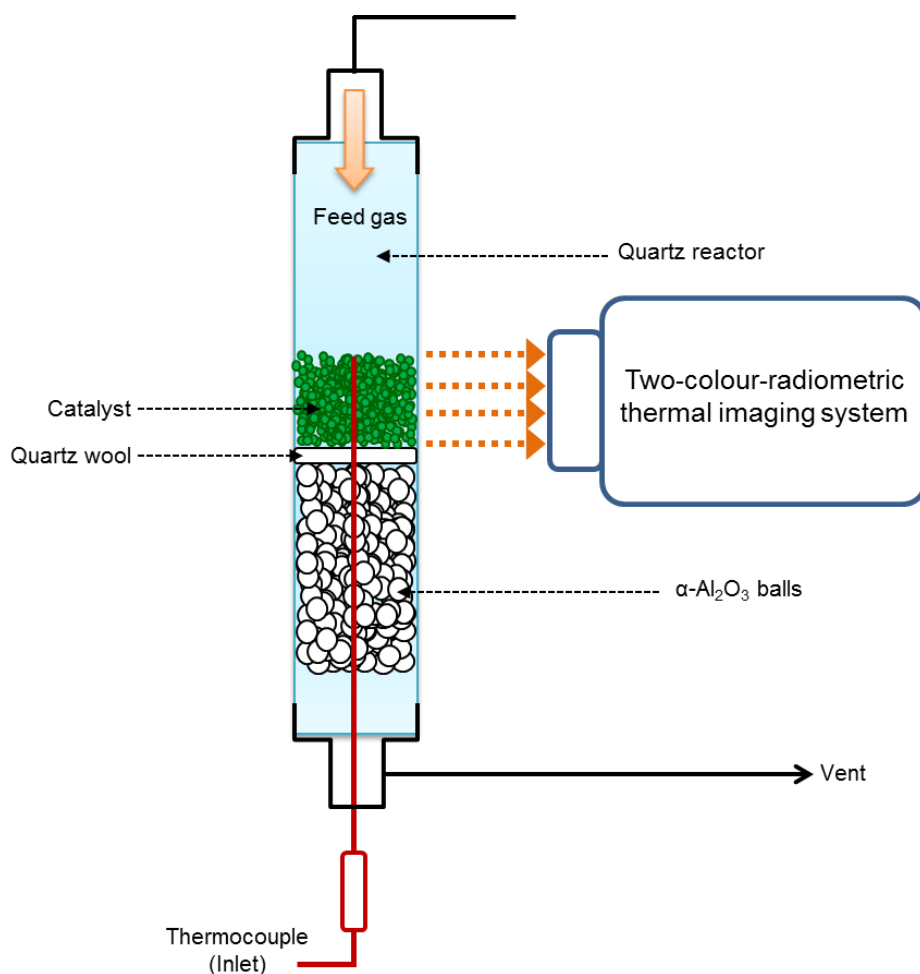


fig. S5. Experimental setup for observing the temperature distribution of the catalyst bed.

The temperature distribution of the catalyst bed was observed by two-color radiometric thermal imaging. After adding the feed gas to the pretreated $\text{RuO}_2/\gamma\text{-Al}_2\text{O}_3$, oxidative decomposition of ammonia was triggered. We then waited 300 s for the gas formation rates to stabilize before acquiring three images sequentially. The exposure times varied because the optimum exposure time was dependent on the temperature of the object. The three images were overlaid, as shown in Fig. 2C.

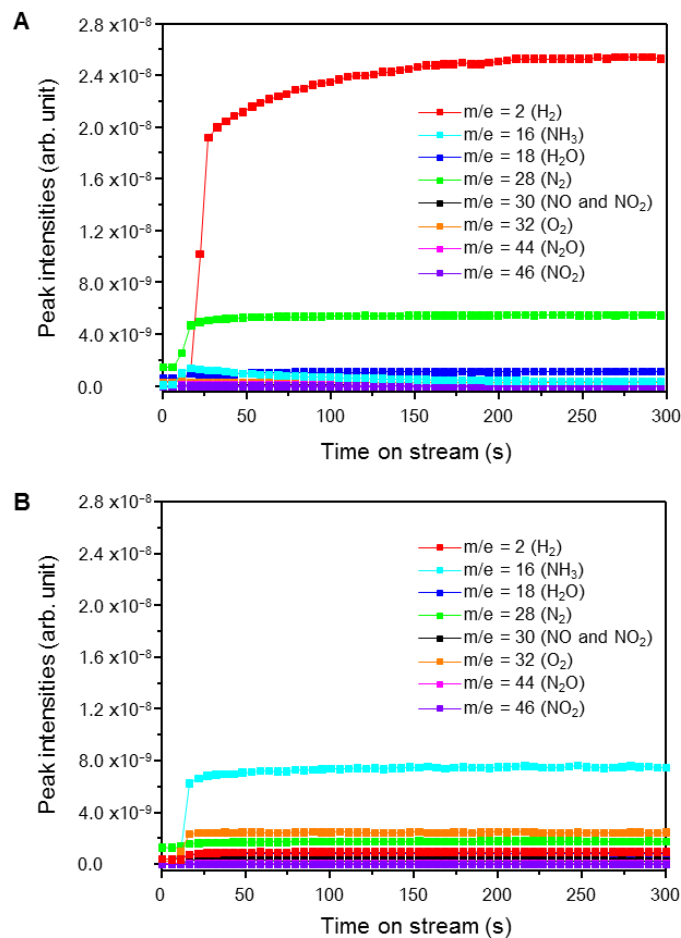


fig. S6. Trends of MS peak intensities during triggering tests over $\text{RuO}_2/\gamma\text{-Al}_2\text{O}_3$ (A) and bare $\gamma\text{-Al}_2\text{O}_3$ (B). The catalysts were pretreated in pure He at 300 °C and then cooled to room temperature (~ 25 °C) under He. Triggering tests were then carried out under quasi-adiabatic conditions (fig. S4). A gaseous mixture of $\text{NH}_3/\text{O}_2/\text{He}$ ($\text{NH}_3:\text{O}_2:\text{He}$ ratio = 150:37.5:20.8 mL min^{-1}) with a GHSV of $62.5 \text{ L h}^{-1} \text{ g}_{\text{cat}}^{-1}$ was supplied at room temperature to the catalyst (fig. S3).

During the triggering tests with $\text{RuO}_2/\gamma\text{-Al}_2\text{O}_3$ (fig. S6A), the composition of the exit gas was constantly monitored with a quadrupole mass spectrometer connected to the exit port of the reactor. For comparison, the results for bare $\gamma\text{-Al}_2\text{O}_3$ are shown in fig. S6B. The mass spectrometry peak intensities for O_2 and ammonia increased after approximately 5 s over $\gamma\text{-Al}_2\text{O}_3$, indicating that the feed gas reached the catalyst. Additionally, over the same time (5 s), formation of N_2 was observed over $\text{RuO}_2/\gamma\text{-Al}_2\text{O}_3$. These results suggest that the reaction occurs immediately after the feed gas is supplied to the catalyst. The compounds NO , NO_2 , and N_2O

were not observed in the mass spectrum (fig. S6A). Note that the slight increase in ammonia concentration at the start of the reaction followed by a decrease (fig. S6A) indicates that a small amount of ammonia passed through the reactor.

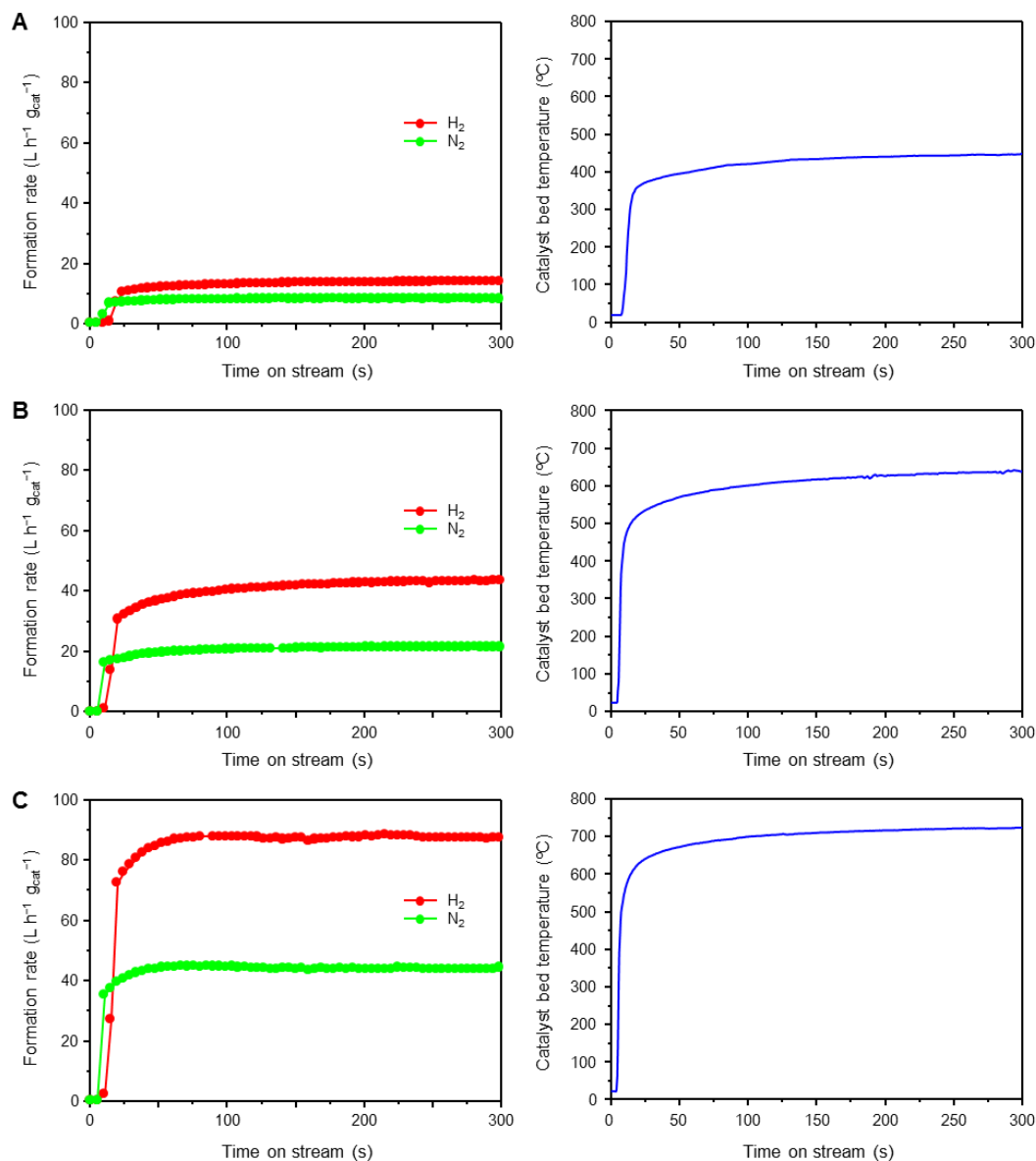


fig. S7. Triggering tests over $\text{RuO}_2/\gamma\text{-Al}_2\text{O}_3$ with three GHSVs. (A) 31.3, (B) 62.5, and (C) $120.8 \text{ L h}^{-1} \text{ g}_{\text{cat}}^{-1}$. Left panels show time dependence of formation rates of H_2 and N_2 , and right panels show temperature at the inlet of the catalyst bed during oxidative decomposition of ammonia. Catalysts were pretreated in He at $300 \text{ }^\circ\text{C}$ for 30 min and cooled to room temperature under He. Then the gaseous mixtures ($\text{NH}_3:\text{O}_2:\text{He}$ ratios of (A) 75:18.8:10.4, (B) 150:37.5:20.8, or (C) 290:72.5:40.2 mL min^{-1}) were supplied at room temperature at the specified rates to a constant weight of catalyst.

Immediately after the feed gases were supplied for all reaction conditions, formation rates of H₂ and N₂ and temperature at the inlet of the catalyst bed increased sharply. These results indicate that oxidative decomposition of ammonia was initiated rapidly. With increase in gas hourly space velocities (GHSV) from 31.3 to 120.8 L h⁻¹ g_{cat}⁻¹, formation rates of H₂ and N₂ increased from 13.5 and 8.0 L h⁻¹ g_{cat}⁻¹ to 87.4 and 44.0 L h⁻¹ g_{cat}⁻¹, respectively. At the same time, the temperature at the inlet of the catalyst bed achieved by the initial rise (20 s) increased from 359 to 624 °C. The conversions of NH₃ and O₂ and yields of H₂ after 30 min are shown in Table S1.

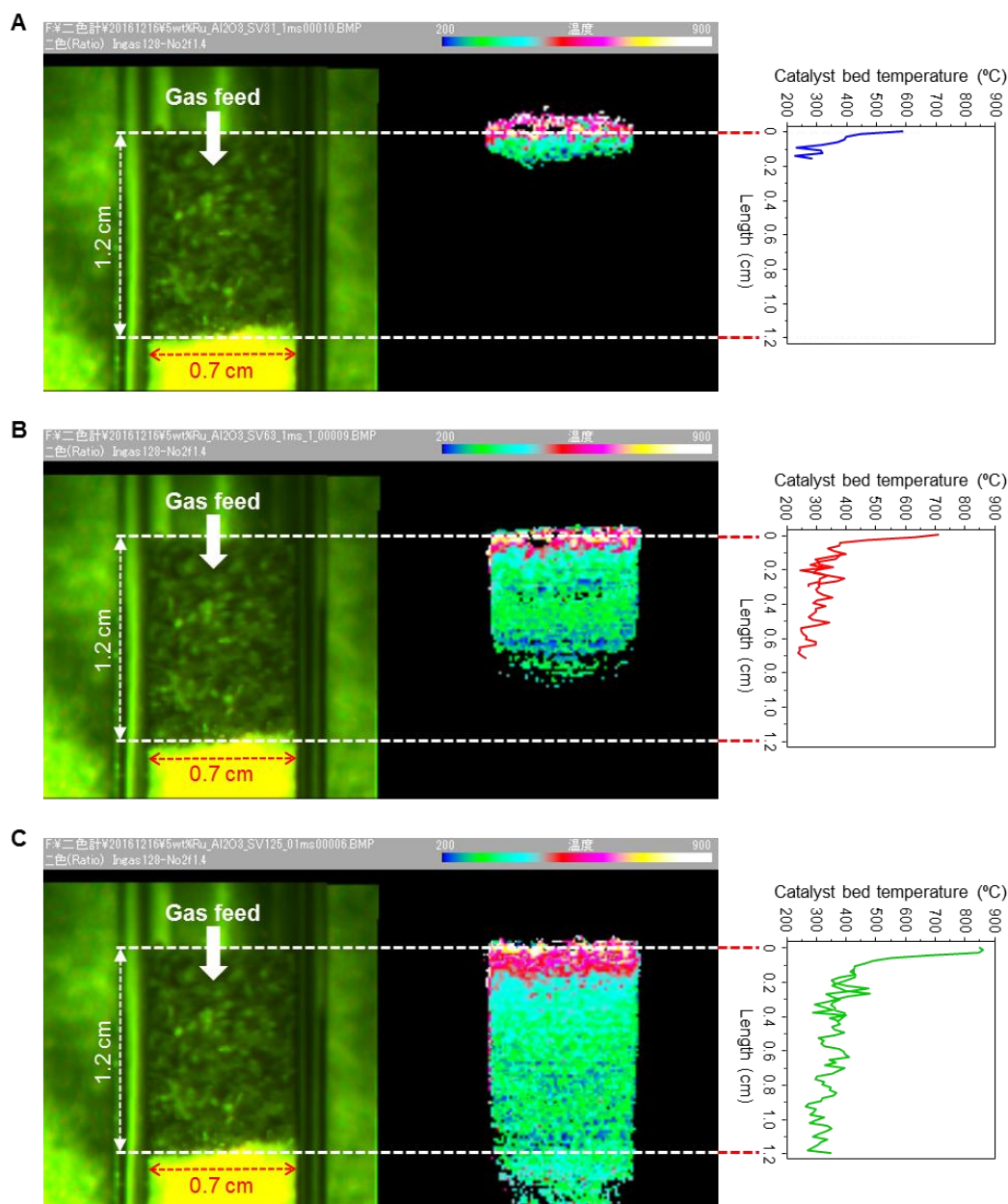


fig. S8. Distribution of catalyst bed temperature measured at 300 s during triggering tests over $\text{RuO}_2/\gamma\text{-Al}_2\text{O}_3$ with three GHSVs. (A) 31.3, (B) 62.5, and (C) 120.8 $\text{L h}^{-1} \text{g}_{\text{cat}}^{-1}$. Catalysts were pretreated in He at 300 °C for 30 min and cooled to room temperature under He. Then the gaseous mixtures ($\text{NH}_3:\text{O}_2:\text{He}$ ratios of (A) 75:18.8:10.4, (B) 150:37.5:20.8, or (C) 290:72.5:40.2 mL min^{-1}) were supplied at room temperature at the specified rates to a constant weight of catalyst.

With the increase in GHSV, at 300 s the high-temperature region (>200 °C) of the catalyst bed had broadened and the maximum temperature increased. These results indicate that heat produced through ammonia combustion (Eq. 3) increased with increase in flow rate, thus increasing catalyst bed temperature.

table S1. Conversions of ammonia and oxygen and yields of hydrogen during triggering tests over RuO₂/γ-Al₂O₃ at three GHSVs.

GHSV (L h ⁻¹ g _{cat} ⁻¹)	Feed gas composition (mL min ⁻¹)	Conversion (%)		H ₂ yield (%)
		NH ₃	O ₂	
31.3	75:18.8:10.4	71	100	40
62.5	150:37.5:20.8	96	100	64
120.8	290:72.5:40.2	100	100	67

We carried out triggering tests for the oxidative decomposition of ammonia (Eq. 2) with three flow rates of gas mixture, 104.2 to 402.7 mL min⁻¹, with 200 mg of the catalyst.

With increase in GHSV, NH₃ conversion and H₂ yield increased; at all GHSVs, O₂ was consumed completely. These results indicate that heat generated through ammonia combustion (Eq. 3) increased with increase in flow rate and this heat was effectively used for endothermic ammonia decomposition (Eq. 1).

table S2. Proportions of NH₃ and O₂ converted and percentage yields of hydrogen during triggering tests over RuO₂/γ-Al₂O₃ with various NH₃/O₂ molar ratios in the feed gas.

NH ₃ :O ₂ (molar ratio)	Feed gas composition (mL min ⁻¹)	Maximum H ₂ yield (%)*	Conversion (%)		H ₂ yield (%)
	NH ₃ :O ₂ :He ratio		NH ₃	O ₂	
4:1.5	150:56.3:2.0	51	100	100	49
4:1	150:37.5:20.8	67	96	100	64
4:0.38	150:14.3:44.0	88	27	100	14

*Calculated assuming stoichiometric reaction of ammonia and O₂ in the feed gas, where some of the hydrogen atoms in the ammonia are consumed to form H₂O. We carried out triggering tests for the oxidative decomposition of ammonia with various feed gas compositions; the total flow rate (208.3 mL min⁻¹) and the flow rate of ammonia (150 mL min⁻¹) were kept constant. For all the investigated conditions, the temperature of the catalyst bed increased immediately after the feed gas was supplied. Consumption of ammonia and O₂, and formation of hydrogen were measured by gas chromatography after 30 min.

These results indicate that the oxidative decomposition of ammonia was triggered successfully, even when the feed gas compositions changed.

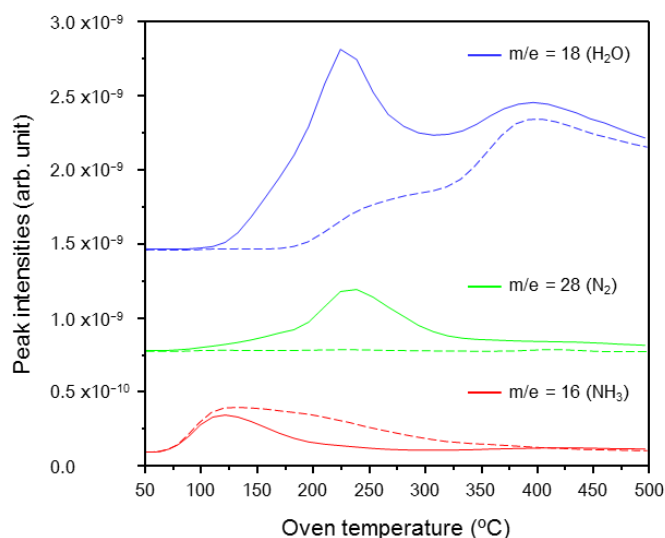


fig. S9. NH₃-TPD profiles of RuO₂/γ-Al₂O₃ (solid lines) and bare γ-Al₂O₃ (dashed lines).

During the NH₃-TPD, the amount of NH₃ desorbed from RuO₂/γ-Al₂O₃ was smaller than that from γ-Al₂O₃. However, formation of N₂ and H₂O were observed over the RuO₂/γ-Al₂O₃ catalyst from about 90 and 100 °C, respectively. In contrast, H₂O was formed above about 170 °C, but N₂ formation was not observed at any temperature range for bare γ-Al₂O₃. These results indicate that a part of the NH₃ adsorbed on RuO₂/γ-Al₂O₃ reacted with O²⁻ in RuO₂ and that N₂ and H₂O were produced.

table S3. Physicochemical properties of the catalysts.

Catalyst	Specific surface area (m ² g _{cat} ⁻¹)	CO adsorbed (μmol g _{cat} ⁻¹)
RuO ₂ /γ-Al ₂ O ₃	156	477
RuO ₂ /La ₂ O ₃	23	23

Reaction: $\text{NH}_3:\text{O}_2:\text{He}$ ratio = 150:37.5:20.8 mL min^{-1} (Total flow: 208.3 mL min^{-1}), 35 min
Purge: Pure He, 60 min

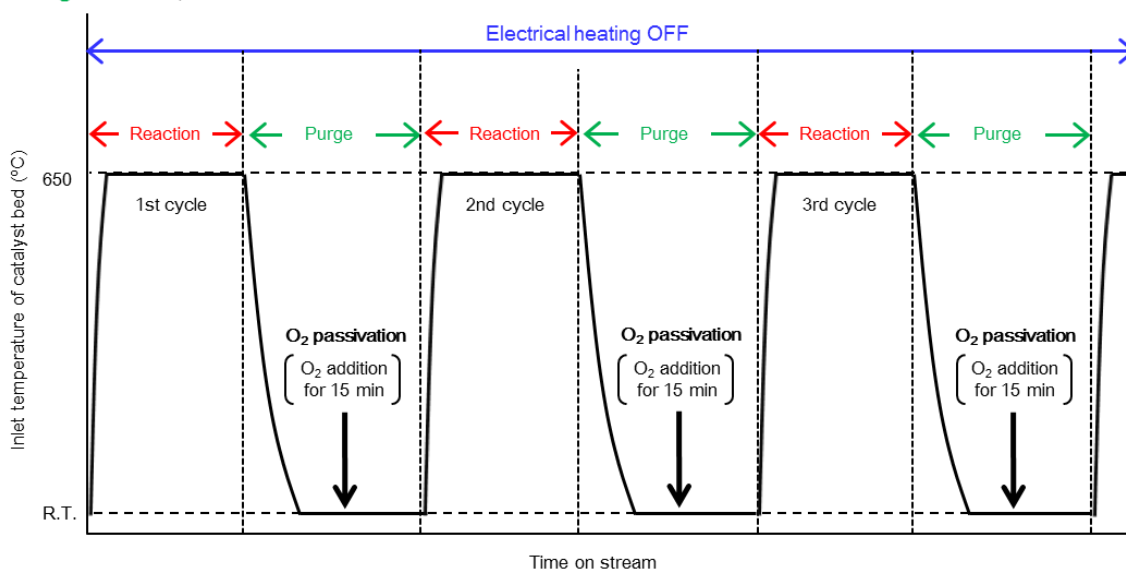


fig. S10. Experimental procedure used for five cycles of testing.

The first cycle was conducted as shown in fig. S3. After 35 min, the reaction was terminated by substituting the $\text{NH}_3/\text{O}_2/\text{He}$ mixture with He, and the catalyst was cooled to room temperature. Then, O_2 was added over the catalyst to oxidize the Ru^0 formed during the reaction in the first cycle. Addition of O_2 to the catalyst eliminated the contribution of the heat produced by Ru^0 oxidation during the next exposure of the reactant to the catalyst (second cycle), that is, O_2 passivation occurred. The $\text{NH}_3/\text{O}_2/\text{He}$ mixture was then supplied to the catalyst. This purge-feed sequence was repeated three more times.

table S4. Molar ratio of Ru/Al in $\text{RuO}_2/\gamma\text{-Al}_2\text{O}_3$ before testing (untreated), after five cycles of testing, and after long-term testing (100 hours).

Testing protocol	Ru:Al (molar ratio)
Untreated	0.031:1
Five cycles of testing	0.030:1
Reaction for 100 h	0.032:1